ORIGINAL PAPER

Optimizing pyrolysis process parameters of plastic grocery bag, with mass–energy assessment and characterization of oil at optimal condition

Dipankar Saha[1] · Jackson Gurung[2] · Bidesh Roy[1] · Ajmal Koya Pulikkal[2] · Abhijit Bhowmik[3] · Satyajit Pattanayak[1,4]

Abstract

The widespread usage of plastic grocery bags, as well as their non-biodegradability, has turned out to be a stern reason for waste generation. With regard to plastic grocery bag disposal, pyrolysis is an encouraging solution that addresses the energy crisis issue as well. This study examined the interactive influences of pyrolysis temperature, residence time, and nitrogen flow for plastic grocery bag pyrolysis to optimize waste plastic oil yield by the Grey–Fuzzy–Taguchi method. Additionally, mass–energy assessment and characterization were done for the waste plastic oil, extracted at the optimal parametric condition. The optimal parametric combination was: temperature 400 °C, time 360 min, and nitrogen flow rate 20 ml/min. The liquid yield at optimal condition was 78.57%, and a minimal error (2.53%) between the predicted and experimental grey fuzzy grade was observed. The oil achieved at optimal condition showed a high hydrocarbon content with a higher heating value of 46,685 kJ/kg. The values of mass ratio, energy ratio, energy efficiency, and energy consumption ratio for the liquid oil were 0.79, 0.89, 0.63, and 0.47, respectively, which indicate the energy favorability for plastic grocery bag pyrolysis. FT-IR results demonstrated mainly the existence of alkene and alkane functional groups in the waste plastic oil. GC–MS results revealed that the oil contains mainly light and middle fractions of 26.4% and 62.7%, respectively, with a smaller proportion (10.9%) of heavy fraction. Finally, the optimum parametric combination can be considered a useful condition for extracting quality fuel from plastic grocery bags.

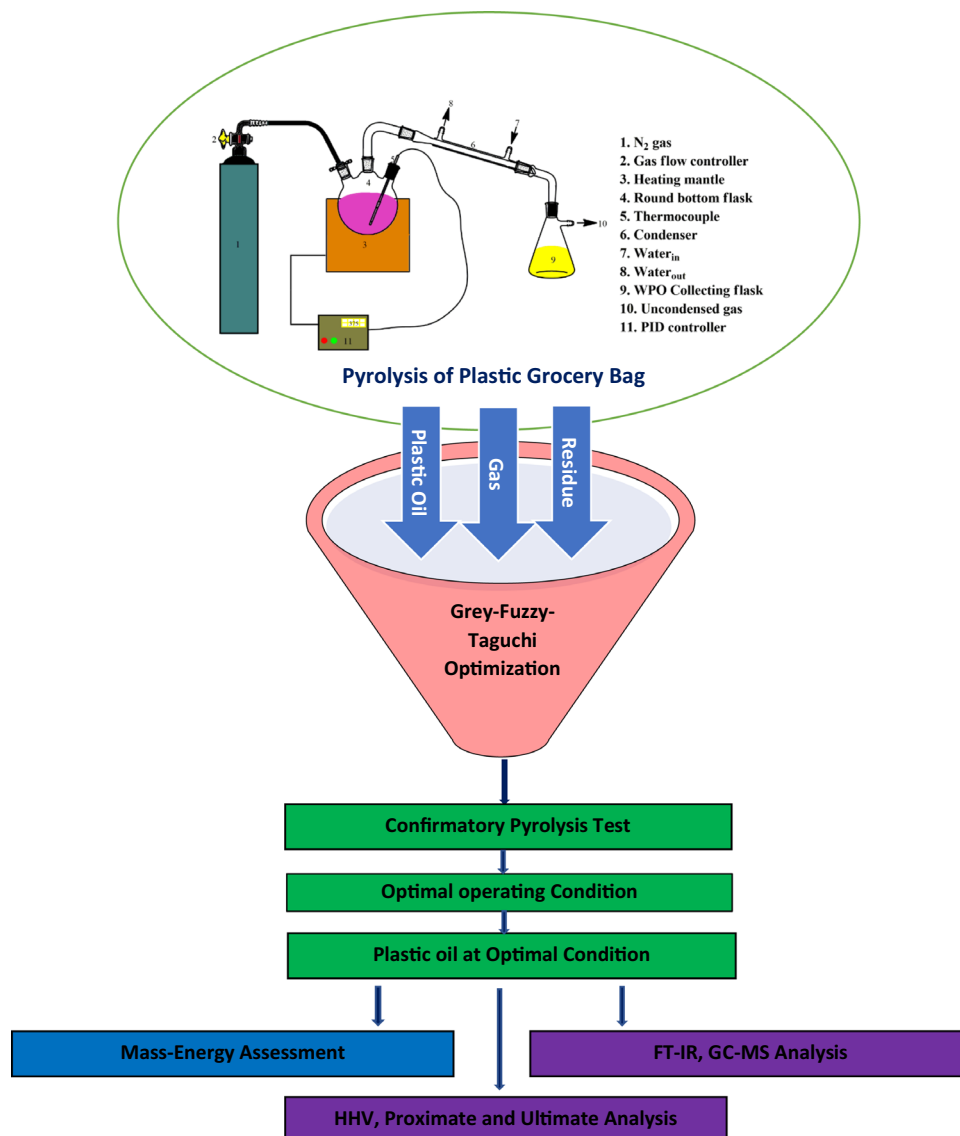✉ Dipankar Saha
   dip2k72013@gmail.com

1   Department of Mechanical Engineering, National Institute of Technology Mizoram, Aizawl 796012, India

2   Department of Chemistry, National Institute of Technology Mizoram, Aizawl 796012, India

3   Department of Mechanical Engineering, National Institute of Technology Agartala, Agartala 799046, India

4   Present Address: Department of Mechanical Engineering, Madanapalle Institute of Technology and Science, Madanapalle 517325, India

Graphical abstract

1. N₂ gas
2. Gas flow controller
3. Heating mantle
4. Round bottom flask
5. Thermocouple
6. Condenser
7. Water$_{in}$
8. Water$_{out}$
9. WPO Collecting flask
10. Uncondensed gas
11. PID controller

Pyrolysis of Plastic Grocery Bag

Plastic Oil · Gas · Residue

Grey-Fuzzy-Taguchi Optimization

Confirmatory Pyrolysis Test

Optimal operating Condition

Plastic oil at Optimal Condition

Mass-Energy Assessment

FT-IR, GC-MS Analysis

HHV, Proximate and Ultimate Analysis

Keywords Grey–Fuzzy–Taguchi · Optimization · Plastic grocery bag · Pyrolysis · Waste plastic oil

Introduction

The plastic industry has seen a gigantic growth in the last few decades, with a huge share of polythene (PE), polypropylene (PP), polystyrene (PS), polyethylene terephthalate (PET), and polyvinyl chloride (PVC), due to its advantages over its counterparts. Different sectors are responsible for the growth in plastic production, but primarily, the packaging industry contributes the most. In 2015, the packaging industry produced approximately 146 million tons of plastic, which is around 36% of the total plastic production worldwide (Our World in Data 2018). The contribution of PE, PP, and PS is approximately 70% of the total produced packaging plastic, PE being the predominant one with 63% contribution (Singh et al. 2019). In line with this, most of the PE is used for making plastic grocery bags (PGB) due to their advantages like durability, flexibility, lightweight, cost-effectiveness, less prone to ripping, water-resistance, and ease of handling. These facts made PGB an appropriate choice for the customers of meat markets, vegetable shops, and of-course grocery shops, and PGB is also extensively used for many other purposes. The production rate of PGB is 160,000 per second, which would be equivalent to 5 trillion by the end of 2021 (The world counts 2021). The rising

usage of PGB has resulted in massive waste generation, with the consequences discernible through terrestrial ecological contamination. The seriousness can likewise be perceived by the measurement of around 5–6 PGBs per foot of the coastline (Dauvergne 2018). In a wider view, the volume of plastic that accumulates in the sea each year is roughly comparable to a truckload of plastic entering the sea per minute (Saha et al. 2021a). A total of 34.50 million tons of waste plastic was generated in the USA in 2015; 75.4% of that was disposed to the dumpsites (Singh et al. 2019), in the same year Europe produced 58 million tons (EUNOMIA. 2018). In India, per day estimation of plastic waste generation is approximately 15,342 tons (CPCB. 2018) with a growth of 10.5% each year in plastics production. Thus, waste management became a genuine worry due to this immense increased production, and the absence of systematized disposal methods. The major factors of such waste creation include industrialization, environmental legislation, economic standing, degree of education, and citizens' understanding of effective waste disposal (Singh et al. 2020). Considering the facts of plastic waste generation, and the production rate and utility level of PGB, the utmost important obligation from an ecological standpoint is the disposal of PGB.

With regard to plastic waste disposal, the commonly followed practices are landfilling and incineration. However, given the non-biodegradability nature of plastic, landfilling is not a viable option, whereas incineration results in hazardous and dangerous contaminations (Saha et al. 2021a). Besides, because plastics are viewed as an energy source, the two strategies eventually result in energy loss (Sharma et al. 2014). Apart from the problems associated with plastic disposal, one more global issue that must be tackled concurrently is the energy crisis caused by the depletion of fossil fuels. Pondering about these real factors, plastic pyrolysis has attained excessive attention lately (Zhang et al. 2020). Pyrolysis yields three products: solid, liquid, and gas. The yields rely upon the sorts of plastic taken as the feedstock, additionally, on the process parameter selected (Kalargaris et al. 2017). Several studies have established and highlighted the aptness of the pyrolysis process for waste plastic treatment (Saha et al. 2021a; Singh et al. 2020). Thus, pyrolysis of plastic is seen as an encouraging solution to the waste-recycling issue (Quesada et al. 2019a), additionally, this process converts the plastic waste into valuable fuel for running internal combustion engines (Saha et al. 2021b).

Because of its adaptability and flexibility, the pyrolysis process may be carried out under a variety of working conditions to enhance the yield and quality based on preference (Zhang et al. 2020). It is noteworthy to mention that the distribution of pyrolysis products is determined by the operating conditions, such as temperature, residence time, and carrier gas flow rate (generally nitrogen). The pyrolysis temperature is considered to be one of the most important

parameters (Sharuddin et al. 2016). Onwudili et al. (2009) and Insura et al. (2010) conveyed that the virgin low-density PE can be pyrolyzed at 425 °C with a liquid yield of 89.5%. Tiikma et al. (2007) found maximum waste plastic oil (WPO) yield at 450 °C. Other researchers (Quesada et al. 2019a; Rodríguez-Luna et al. 2021) also performed PE pyrolysis in a temperature range of 450–550 °C and found that the temperature for the maximum WPO-yield was 500 °C. Whereas, Kalargaris et al. (2017) pyrolyzed PE at a high temperature of 700℃. However, Sharuddin et al. (2016) reported that for the production of WPO, suitable temperatures are less than 500℃. Venkatesan et al. (2018) performed the pyrolysis of PE at 350–425 °C. Geo et al. (2018) also performed the experiment with PE at a lower temperature (376–420 °C) and achieved a WPO yield of 75%. Likewise, other researchers (Geo et al. 2018; Bharathy et al. 2019) have also done the pyrolysis of PE-based plastics for WPO production, and the WPO yields ranged between 43 and 80%. The residence time is connected to the duration of the experiment at the target temperature (Pan et al. 2021). It is also an important factor in influencing the yield composition (Onwudili et al. 2009). Quesada et al. (2019a, b) reported that an extended residence time might enhance the WPO yield. In another study (Muhammad et al. 2018), the influence of nitrogen flow rate (ranging in 0–60 mL/min) on PE pyrolysis was investigated and it was observed that gas flow rate also influences the product distribution of PE pyrolysis. The yield of WPO can be increased by the increment in the gas flow rate while decreasing the yield of solid residue (Pan et al. 2021).

From the literature, it has been observed that various studies on plastic pyrolysis have been conducted to examine the impacts of the operating variables on the WPO-yield. But, the bulk of the studies was either focused on investigating such impacts by altering the individual operating parameters one by one, keeping other parameters constant; or simply, the experiments were carried out at a single set of operating conditions to determine the WPO-yield. However, operational conditions of plastic pyrolysis have very complicated interactive effects on WPO generation; thus, individual parametric interaction is not a convincing strategy particularly for evaluating the WPO-yield. This requires establishing a multiparametric optimization (Quesada et al. 2019a), which is seldomly reported in the literature (in the context of WPO-yield). Additionally, to the best of the authors' knowledge, optimization of PGB pyrolysis for WPO-yield is yet to be reported. In such circumstances of multiparametric optimization, various techniques can be implemented such as response surface methodology (RSM), artificial neural network (ANN), Taguchi-based Grey relational analysis (GRA), fuzzy logic, etc. RSM does not deal accurately with nonlinearity and imprecise data and requires the order of the model to be stated. But ANN outperforms

RSM as a better modeling method owing to its capability of establishing nonlinear relationships and effective data representation without any intricacy. However, ANN considers training data and provides impenetrable, opaque models (Khamparia et al. 2020). In this regard, Taguchi-based GRA has gained prominence in several fields of research (Panda et al. 2016). Though individually, Taguchi is not suitable for multiparametric optimization, it provides a lesser number of experiments (design of experiments), the response variable of which can be applied in other optimization techniques. Based on the information of the response variables acquired from the lower number of experimental runs, GRA can be applied for an effective multi-parametric optimization (Jozić et al. 2015). In Taguchi-based GRA, all the experiments can be ranked based on Grey relational grade (GRG) and the influencing factors can also be determined. However, Taguchi-based GRA has its innate incapacity to differentiate information domains based on the quantitative or qualitative nature amongst the ideal cases of a unique solution or no solution; thus, Taguchi-based GRA fails to deliver a robust result. To overcome the above-stated limitations of simple Taguchi-based GRA, fuzzy logic can be coupled with it which is called the Grey–Fuzzy–Taguchi technique (Roy et al. 2016). Fuzzy logic is attractive owing to its effortlessness and ease in dealing with vagueness, imprecise, and uncertain data. It can easily merge with other control methods based on the usage of natural language-related methods (Khamparia et al. 2020). The fuzzy logic is an intelligent decision-making tool and it takes decisions according to non-numerical and indefinite information (Paramasivam 2020). Thus, the Grey–Fuzzy–Taguchi technique becomes a uniquely robust and viable solution for multiparametric optimization problems (Roy et al. 2016).

In brief, the extensive usage of PGBs and also their non-biodegradability, has turned out to be a stern reason for waste generation. Regarding the disposal of PGB, pyrolysis is a promising solution that also addresses the issue of energy crisis. This present investigation aims to optimize the PGB pyrolysis parameters to maximize the WPO-yield. As individual parametric interaction is not a convincing strategy, the multiparametric optimization technique Grey–Fuzzy–Taguchi has been applied to optimize the PGB pyrolysis parameters (temperature, residence time, and nitrogen flow rate) to maximize the WPO-yield while minimizing gas and solid residue. This study provides a first-of-a-kind insight into the possibility of the application of the Grey–Fuzzy–Taguchi technique in the optimization of PGB pyrolysis parameters to achieve a robust optimal parametric combination. The WPO extracted at the optimal parametric condition was characterized by FT-IR (Fourier-transform infrared spectroscopy) and GC–MS (gas chromatography-mass spectrometry). Additionally, proximate and ultimate analysis was carried out for the WPO (obtained at

the optimal condition), and the higher heating value (HHV) was also determined. Further, mass–energy assessment has been done for the WPO-yield obtained at the optimum operating condition.

Materials and methods

Materials and characterization

The material employed in this investigation is PGB which is frequently used for a variety of reasons such as carrying grocery items, meats, vegetables, etc. PGBs were obtained from the local market of Aizawl, India. Proximate analysis was carried for PGB following ASTM standards (Cai et al. 2017) to estimate the contents of moisture, volatile, ash, and fixed carbon. The reported results related to the proximate analysis were the average of three experiments. Ultimate analysis was done using Elemetar Vario EL III to estimate the elemental composition (carbon, hydrogen, nitrogen, sulfur, and oxygen). Proximate and ultimate analysis was also done for the WPO achieved at the optimal operating conditions. Higher heating values of PGB and WPO were determined by Labtronics Automatic Bomb Calorimeter. Apart from that, FT-IR and GC–MS analyses were also carried out for WPO using PerkinElmer spectrum two (8300–350 cm^{-1}), and Agilent 7890A GC with 5975C mass spectrometer, respectively.

Experimental setup

The pyrolysis experiments for the PGB were performed at the National Institute of Technology Mizoram, India. The schematic of the pyrolysis setup is illustrated in Fig. 1. The reactor is a three-neck round-bottom flask of 2 L capacity. Through one neck, N_2 was provided in order to make an inert environment, the second neck was connected with the condenser by an adapter, and a K-type thermocouple was inserted through the other neck which touches the inner base of the flask. A heating mantle of 400 W was used for this study which was PID controlled. In each experiment, 500 gm of PGB was taken as feed, initially, the flask was purged with N_2 with a flow rate of 100 ml/min for 10 min for ensuring the inert environment inside the flask. The flow rate was adjusted at the corresponding target pyrolysis temperature for a specific residence time for PGB in the round-bottom flask as per the design of experiments. The volatile gas evolved during the PGB pyrolysis was vented through the condenser where it got converted into the liquid form, and thus, WPO was collected in the 500-ml conical flask as shown in Fig. 1. The water which was circulating through the condenser was maintained at 5–8 °C. The remaining solid residue content in the round-bottom flask was collected
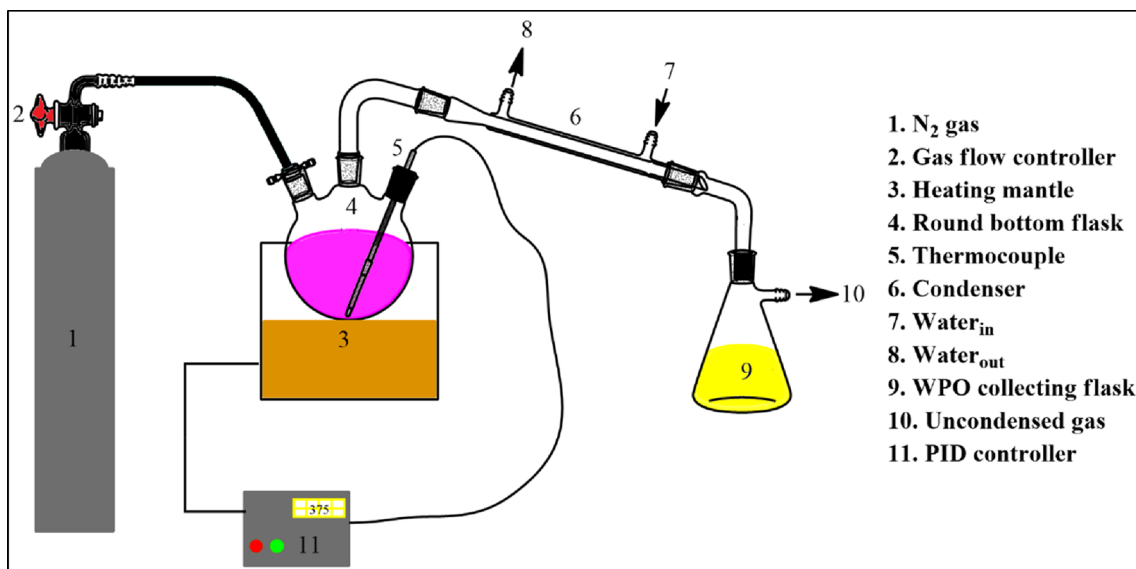
Fig. 1 Schematic diagram of experimental setup

Table 1 Experimental factors and their levels

Process parameters		Level 1	Level 2	Level 3	Level 4
Temperature (℃)	A	325	350	375	400
Time (min)	B	180	240	300	360
N_2 flow rate (ml/min)	C	10	20	30	40

Table 2 Design of experiment using Taguchi orthogonal array (L16)

Test	A	B	C
1	1	1	1
2	1	2	2
3	1	3	3
4	1	4	4
5	2	1	2
6	2	2	1
7	2	3	4
8	2	4	3
9	3	1	3
10	3	2	4
11	3	3	1
12	3	4	2
13	4	1	4
14	4	2	3
15	4	3	2
16	4	4	1

at the end of each experiment, and the weight was measured after the flask was cooled down.

Design of experiments

In this present study, a Taguchi-based L-16 orthogonal array (using Minitab-20 software) was used for the design of experiments which was based on three factors and four levels. Pyrolysis temperature, residence time, and N_2 flow rate are the three factors. The temperature was varied from 300 to 400 °C, the residence time was varied from 180 to 360 min, and the N_2 flow rate was altered from 10 to 40 ml/min. The details of the process parameters/factors and their levels can be found in Table 1. The 16 combinations of all the factors and their levels are shown in Table 2. The detailed experimental layout and yields can be found in Table 3. The yields (shown in Table 3) for each parametric condition are the average of three experimental runs.

Determination of pyrolytic yields

For each experiment, a total of 500 gm (W) of PGB was taken. The weight of the WPO (W_L) was measured by subtracting the weight of the initially measured empty collecting

(conical) flask. Similarly, the final weight of the round-bottom flask was measured after each experiment which contains the solid residue. Then the weight of the initial empty round-bottom flask was subtracted to get the weight of the solid residue (W_S), and the weight of the uncondensed gas (W_G) was calculated as

$$W_G = W - W_L - W_S \tag{1}$$

The corresponding percentages of the yields of WPO (Y_L), solid residue (Y_S), and uncondensed gas (Y_G) can be calculated by the following Eqs. (2–4) (Quesada et al. 2019a)

Table 3 Experimental layout and response variables for pyrolysis yields

Test	Process variables			Response variables		
	A	B	C	$Y_L(\%)$	$Y_S(\%)$	$Y_G(\%)$
1	325	180	10	55.06	34.08	10.86
2	325	240	20	52.8	31.28	15.92
3	325	300	30	60.02	24.98	15
4	325	360	40	66	19.48	14.52
5	350	180	20	46.06	40.88	13.06
6	350	240	10	55.32	31.34	13.34
7	350	300	40	61.54	26.48	11.98
8	350	360	30	69.28	18.66	12.06
9	375	180	30	55.54	33.08	11.38
10	375	240	40	61.32	30.32	8.36
11	375	300	10	71.36	21.3	7.34
12	375	360	20	77.54	15.54	6.92
13	400	180	40	57.56	33.3	9.14
14	400	240	30	65.48	27.38	7.14
15	400	300	20	74.32	19.62	6.06
16	400	360	10	76.06	17	6.94

$$Y_L = \frac{W_L}{W} \times 100 \tag{2}$$

$$Y_S = \frac{W_S}{W} \times 100 \tag{3}$$

$$Y_G = \frac{W_G}{W} \times 100 \tag{4}$$

The experimental layout and the corresponding yields (response variables) are shown in Table 3.

Grey–Fuzzy–Taguchi method

Grey relational analysis (GRA)

A Grey system is one in which some of the information is known, but the rest is unknown (Jozić et al. 2015). Because there is always ambiguity, the Grey system provides a choice of potential solutions. Based on this theory, GRA may be efficiently applied for addressing the complex interrelationships among the designed performance characteristics. In GRA, the GRG is favorably defined which is an indicator of multiple performance characteristics. In recent times, GRA has evolved into a robust tool to analyze processes with multiple performance characteristics (Pandey et al. 2018). GRA condenses complex multiple response variables into a single response GRG. The detailed method for calculating the GRG is explained below:

Data processing

Data processing is accomplished to convert the original sequence into a similar comparable sequence. The yields' numerical values can be normalized between 0 and 1. In this study, for normalization, two approaches are followed which are larger-the-better and smaller-the-better. For Y_L larger-the-better approach has been followed whereas, for Y_S and Y_G smaller-the-better approach has been followed. The following Eqs. (5–11) are used for this purpose (Jozić et al. 2015).

Larger-the-better:

$$x_{ij} = \frac{y_{ij} - \min(y_{ij})}{\max(y_{ij}) - \min(y_{ij})} \tag{5}$$

Smaller-the-better:

$$x_{ij} = \frac{\max(y_{ij}) - y_{ij}}{\max(y_{ij}) - \min(y_{ij})} \tag{6}$$

where y_{ij} is the initial sequence of jth response in the ith experiment and x_{ij} is the corresponding normalized value.

After considering a larger or smaller-the-better approach followed by normalization, the response variable which has a normalized value equal to 1 is considered to be the best one and accordingly, the deviation sequence for each response variable for all the experiments are found by subtracting the corresponding values from 1. The reference sequence x_{0j} for jth response is $(x_{01}, x_{02}, \ldots x_{0j}) = (1, 1, 1, \ldots, 1)$. Then, Grey relational coefficient (GRC: $\Upsilon(x_{0j}, x_{ij})$) is evaluated for x_{ij} to determine how close the x_{ij} is w.r.t x_{0j}, the following Eqs. are used for this purpose:

$$\Upsilon\left(x_{0j}, x_{ij}\right) = \frac{\Delta_{\min} + \xi\Delta_{\max}}{\Delta_{ij} + \xi\Delta_{\max}} \tag{7}$$

where $\Upsilon\left(x_{0j}, x_{ij}\right)$ is the GRC between x_{0j} and x_{ij},

$$\Delta_{ij} = \left| x_{0j}, x_{ij} \right| \tag{8}$$

$$\Delta_{\min} = \min\left\{ \Delta_{ij}, i = 1, 2, \ldots m; j = 1, 2, \ldots n \right\} \tag{9}$$

$$\Delta_{\max} = \max\left\{ \Delta_{ij}, i = 1, 2, \ldots m; j = 1, 2, \ldots n \right\} \tag{10}$$

ξ is the distinguishing coefficient, usually it is assumed to be 0.5; thus, in this study also ξ is assumed as 0.5 (Panda et al. 2016). In the next step, GRG is calculated which is nothing but the weighted sum of all the response GRCs of a single experiment. The GRG can be evaluated by the following Eq.:

$$\Upsilon = \frac{1}{n} \sum_{j=1}^{n} \Upsilon\left(x_{0j}, x_{ij}\right) \text{ for } i = 1, 2, \ldots m \tag{11}$$

Then the GRG values are arranged according to descending order, and the highest GRG is ranked 1. The means of GRG (Υ_i) for each level of process variables are found, the larger the mean value of GRG (at each level) is

the better the various performance characteristics (Jozić et al. 2015).

Fuzzy interface system (FIS)

The steps in fuzzy logic include fuzzification, fuzzy rule interface, and defuzzification of crisp value. GRCs are fuzzified with fuzzifier applying membership functions. Then a fuzzy interface was executed by the fuzzy interface engine to form fuzzy rules for a single fuzzy value from the three different GRCs. Further, the single fuzzy value was transformed into a grey fuzzy grade (GFG) using a defuzzifier (Lin and Lin 2005). MATLAB tool has been used for the grey fuzzy technique. Firstly, three different GRCs are transformed into a rhetorical fuzzy set. For fuzzification of GRCs, triangle membership functions have been used by considering large (L), medium (M), and small (S) fuzzy subsets that lead to the distribution of the GRCs between 0 and 1. GFG, the response characteristic of FIS also ranges between 0 and 1 which is transformed by triangle membership functions considering seven different fuzzy subsets viz. VVH (very very high), VH (very high), H (high), M (medium), L (low), VL (very low), and VVL (very-very low). Figure 2 shows various fuzzy subsets adopted, and Fig. 3 depicts the quantity of fuzzy rules executed. IF–THEN rules have been applied for the boundary statement which offered 81 fuzzy

Fig. 2 Triangular function of seven fuzzy subsets (for GFG)
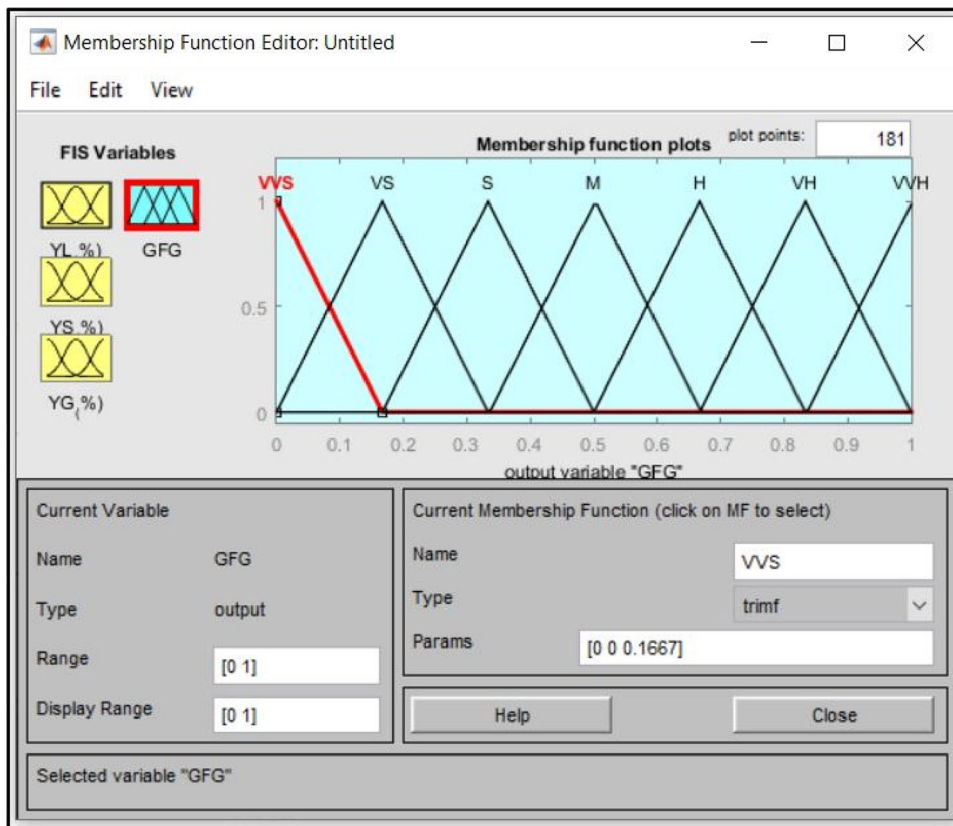
Fig. 3 Fuzzy assisted membership function (for GFG)

logics that obey the following (Bhowmik and Biswas. 2021; Dey et al. 2019):

Rule 1» If β_1 is J_1 and β_2 is K_1 and β_3 is L_1 then x is M_1 else,

Rule 2» If β_1 is J_2 and β_2 is K_2 and β_3 is L_2 then x is M_2 else,

Rule n» If β_1 is J_n and β_2 is K_n and β_3 is L_n then x is M_n else.where β_1, β_2 and β_3 are input fuzzy values; J_n, K_n, L_n and M_n are fuzzy subsets; and x is the response output.

The multi-response fuzzy output with membership function is expressed as:

$$\mu D_i(y_i) = \text{Max}\left[\text{Min}_j\left\{\mu J_{\beta_1}(\beta_1), \mu J_{\beta_2}(\beta_2), \mu J_{\beta_3}(\beta_3) \ldots \mu J_{\beta_n}(\beta_n)\right\}\right] \tag{12}$$

The defuzzification to convert fuzzy interference output $\mu D_i(y_i)$ (Roy et al. 2016) into an un-fuzzy GFG (y^k), can be executed by the following formula:

$$y^k = \frac{\int y_i \mu D_i(y_i) dy}{\int \mu D_i(y_i) dy} \tag{13}$$

A higher GFG (or y^k) provides higher performance characteristics.

Analysis of variance (ANOVA) for GFG

ANOVA has been done in this study to determine the influential level of the controllable parameters. This is performed by separating the total variability of the GFGs, which is calculated by the sum of the squared deviations from the total mean of the GFG into contributions by each controllable

parameter and the error. The contribution percentage of each process parameter in the overall sum of the squared deviations was utilized to assess the significance of a controllable parameter change on the performance characteristic. The ANOVA approach separates the total variability of the response (sum of squared deviations about the grand mean) into the contribution and error of each parameter» The P-value (probability of significance) is usually determined based on the Fisher's ratio or F-value, if its value is less than 0.05, the controllable parameter is significant enough (Panda et al. 2016).

Prediction of optimal GFG

The optimal GFG (Υ_p) is predicted using the following Eq. at the designated optimal controllable variables (Awale and Inamdar. 2020):

$$\Upsilon_p = \Upsilon_t + \sum_{i=1}^{p}(\Upsilon_i - \Upsilon_t) \tag{14}$$

where Υ_p is the predicted GFG of optimal operating condition, Υ_t is the total mean of GFG, Υ_i is the mean of GFG at the optimal level, p is the controllable variable that effects the multiple performance characteristics significantly.

Mass and energy assessment

For mass and energy assessment, WPO-yield was used which was obtained at the optimal condition. A similar approach has been followed in another study (Guo et al.

2017). The necessary Eqs. in this regard are shown below (Guo et al. 2017).

The mass ratio (MR) can be defined as:

$$MR = \frac{M_{WPO}}{M_{RP}} \tag{15}$$

where M_{WPO} is the mass of WPO at the optimal condition and M_{RP} is the mass of raw plastic/feed.

The energy ratio (ER) can be defined as:

$$ER = \frac{M_{WPO} \times HHV_{WPO}}{M_{RP} \times HHV_{RP}} \tag{16}$$

where HHV_{WPO} is the higher heating value of WPO and HHV_{RP} is the higher heating value of raw plastic.

Energy efficiency (η_{ef}) compares the energy contained in the target fuel (in this study, WPO) to that contained in the feedstock, taking into account other energy inputs necessary during the conversion process. The following formula is used to calculate the η_{ef}:

$$\eta_{ef} = \frac{M_{WPO} \times HHV_{WPO}}{M_{RP} \times HHV_{RP} + Q_{input}} \tag{17}$$

where Q_{input} is the electricity consumed (EC) during the pyrolysis process.

The energy consumption ratio (ECR) may be used to evaluate the process's energy balance. The ECR may be attained by dividing the electricity consumed (EC) during the pyrolysis process by the available energy of the target yield, in this case, WPO. If ECR < 1, the reaction is energy beneficial because the target product has higher energy than the energy required for the conversion (Vieira et al. 2020). ECR is calculated as:

$$ECR = \frac{EC}{M_{WPO} \times HHV_{WPO}} \tag{18}$$

FT-IR analysis

FT-IR analysis was done for the determination of the major functional groups in WPO. For this, PerkinElmer spectrum two (8300–350 cm^{-1}) was used. The FT-IR spectra were recorded in the range 4000–400 cm^{-1}, the operating range was 5–45℃, LiTaO$_3$ type of detector and spectrum 10™ software was used for this analysis.

GC–MS analysis

Agilent 7890A GC with 5975C mass spectrometer was used for this analysis which has an HP5-MS column. The initial oven temperature was 55 °C with a hold time of 2 min, and then it was heated up to 300 °C. The injector volume was 1 μl with a split ratio of 50:1 and a split-flow of 50 ml/min. Helium has been used as a carrier gas.

Results and discussion

PGB characterization

Table 4 displays the findings of the proximate analysis and ultimate analysis, as well as the HHV. It is found that the PGB has small moisture and fixed carbon content. Ash percentage is 4.76%, lower ash percentage is advantageous for the pyrolysis process since a low ash level reduces the possibility of fouling. PGB consists of a very high volatile content (94.48 percent), indicating that it is suitable for pyrolysis (Saha et al. 2021a). The high volatile content and low ash content are desired for liquid oil production (Mumbach et al. 2019). The ultimate analysis result shows that the carbon and hydrogen levels in the PGB sample are 73.25% and 12.30%, respectively, indicating that PGB may be transformed into hydrocarbon-rich products. The oxygen concentration of PGB is 9.03 percent (by difference), whereas the nitrogen and sulfur levels are 0.02% and 0.49%, respectively (Saha et al. 2021a). Lower nitrogen and sulfur concentrations are preferable because they reduce the development of oxides of the corresponding elements (Mumbach et al. 2019). PGB has an HHV value of 41,258 kJ/kg.

Table 4 Proximate and ultimate analysis, and HHV of PGB

Proximate analysis (Saha et al. 2021a)	
Content	Weight (%)
Moisture	0.15
Volatile	94.48
Ash	4.76
Fixed carbon*	0.61
Ultimate analysis (Saha et al. 2021a)	
Content	Weight (%)
Carbon	73.25
Hydrogen	12.30
Nitrogen	0.02
Sulphur	0.49
Oxygen*	9.03
HHV	
41,258 in kJ/kg	

*: calculated by difference

WPO yield and optimization by Grey–Fuzzy–Taguchi

The pyrolysis process yielded three pyrolytic products: Y_L, Y_S, and Y_G. Table 3 shows the yields achieved at different sets of parameters. It is seen that the WPO yield varied in the wide range between 46 and 78% approximately. It is also observed that the WPO is strongly dependent on the residence time, at longer residence time the yield of WPO was higher. The 4th, 8th, 12th, and 16th experiments, all having maximum residence time (360 min) in their parametric setting, offered high WPO yields of approximately 66%, 69%, 78%, and 76% respectively, with lower yields of solid residue and gas. It appears that the longer the residence time, the higher the WPO yield, this can also be supported by the study reported by Wirawan and Fariza (2019). In another study also, it was found that residence time has a greater influence when the pyrolysis temperature is below 450 °C (Quesada et al. 2019a). An extended residence time leads to a higher conversion of primary products resulting in hydrocarbon yields of lighter molecular weights (Sharuddin et al. 2016). Compared to residence time, the pyrolysis temperature and nitrogen flow rate showed a slightly lesser influence on the yields. The WPO yield found in this study is comparable to a few other studies, for example, Quesada et al. (2019a) achieved a maximum of 66.5% WPO at 500 °C, Mastral et al. (2002) achieved 80% at 645 °C, and Miskolczi et al. (2004) achieved 75.5% at 450 °C.

Sixteen experiments have been conducted based on the Taguchi L-16 orthogonal array, as mentioned earlier. The experimental layout and the yields of the pyrolysis process are shown in Table 3. All the response variables (yields) are normalized, deviation sequence and GRC have been also evaluated for each experiment as shown in Table 5. Table 5 also shows the GRG values for all the sixteen experiments based on which the experiment numbers were ranked from 1 to 16. The ranking shows that experiment number 12 was the number 1 ranked. Table 6 shows the ranks and corresponding GFG values of the experiments and in this case also it was confirmed that the 12th experiment is ranked 1 with the highest GFG values. Figure 4 depicts the comparison between GRG and GFG values of the sixteen experiments. Figure 5 represents GFG vs temperature, time, and N_2 flow rate profiles for the main effects plot for means and SN ratios. Table 7 is the response table for the main effects for means of GFG. In Table 7, the GFG values for each level are found out for every factor, and the highest or optimal level of each factor is found which is highlighted by bold font. From Fig. 5 and Table 7, it is obvious that for the process variables A, B, and C (temperature, time, and N_2 flow rate, respectively), the optimum levels are 4, 4, and 2, respectively. Therefore, A4-B4-C2 is the optimum operating condition. The total mean of GFG was 0.558. In addition, based on the

descending order (of GFG value) of the optimal levels, the process parameters are ranked, which revealed that within this domain of research, B was the most influencing factor followed by A and C.

Furthermore, ANOVA was also carried out to evaluate the significance level of the process parameters. Table 8 lists out the results of ANOVA. The sum of square values of the factors: temperature, time, and N_2 flow were 0.13449, 0.19515, and 0.015730 respectively, and the F-values of the corresponding parameters were 10.1, 14.66, and 1.18, respectively. The P values for temperature, time, and N_2 flow were found to be 0.009, 0.004, and 0.393, respectively. This establishes that time is the most significant factor followed by temperature, whereas, N_2 flow is the insignificant control factor. The process parameters (temperature, time, and N_2 flow) contributed 36.15%, 52.46%, and 4.23%, respectively, to the response variables.

Confirmatory experiment

The ANOVA results revealed that out of three, two process parameters are significant factors. Based on this information and using Eqs. (14), the GFG was predicted for the optimal parametric condition A4-B4-C2. The predicted GFG was found to be equal to 0.81825. Furthermore, a confirmatory experiment was carried out at the optimal condition. Table 9 shows the results of GFG at the optimum parametric combination (A4-B4-C2). The GFG value of the confirmatory experiment was found to be 0.79751. A negligible error of 2.53% was noticed between the predicted and experimental GFG, which shows a good correlation. Finally, it can be said that a multiparametric optimization was carried out with a good agreement between predicted and actual GFG.

Characterization, and mass–energy assessment of WPO

Proximate analysis, ultimate analysis, HHV, and mass–energy assessment of WPO

The results of proximate analysis, ultimate analysis, and HHV of WPO achieved at optimal operating condition are tabulated in Table 10. From the proximate analysis results, it has been found that WPO contains 99.26% of volatile matter with a very negligible amount of moisture and ash content. This reveals the suitability of WPO for engine application. Whereas, the ultimate analysis results show that the carbon and hydrogen content in WPO is high, 81.38% and 14.50%, respectively. The nitrogen and sulfur contents in WPO are 0.35% and 0.17%, respectively, lower levels of nitrogen and sulfur mean that the chance of

Table 5 Normalization, Deviation sequence, Grey relational coefficients (GRC), and Grey relational grades (GRG) of the experimental results

Test	Normalization			Deviation sequence			Grey relational coefficients (GRC)			Grey relational grades (GRG)	Rank
	Y_L	Y_S	Y_G	Y_L	Y_S	Y_G	Y_L	Y_S	Y_G		
1	0.285896	0.26835043	0.51318458	0.714104193	0.731649566	0.486815	0.411826	0.40595963	0.50668	0.441488756	12
2	0.214104	0.37884767	0	0.785895807	0.621152328	1	0.388834	0.44596973	0.333333	0.389379018	15
3	0.443456	0.62746646	0.09330629	0.556543837	0.372533544	0.906694	0.473241	0.57304387	0.355443	0.467242802	11
4	0.633418	0.8445146	0.14198783	0.366581957	0.155485399	0.858012	0.576979	0.7627935	0.368185	0.569319394	7
5	0	0	0.29006085	1	1	0.709939	0.333333	0.33333333	0.413244	0.359970197	16
6	0.294155	0.37647987	0.26166329	0.705844981	0.623520126	0.738337	0.414647	0.44502986	0.403767	0.421148086	14
7	0.491741	0.56827151	0.39959432	0.508259212	0.431728493	0.600406	0.495904	0.53663702	0.454378	0.495639707	9
8	0.737611	0.87687451	0.39148073	0.262388818	0.123125493	0.608519	0.655833	0.80240659	0.451052	0.63643069	5
9	0.301144	0.30781373	0.46044625	0.698856417	0.692186267	0.539554	0.417064	0.41939755	0.480976	0.439145761	13
10	0.484752	0.41673244	0.76673428	0.515247776	0.583267561	0.233266	0.492491	0.46156648	0.681881	0.545312716	8
11	0.803685	0.7726914	0.87018256	0.196315121	0.227308603	0.129817	0.718066	0.68746609	0.793881	0.73313754	4
12	1	1	0.9127789	0	0	0.087221	1	1	0.851468	0.950489349	1
13	0.365311	0.29913181	0.68762677	0.634688691	0.700868193	0.312373	0.440649	0.41636543	0.615481	0.490831858	10
14	0.6169	0.53275454	0.89046653	0.383100381	0.467245462	0.109533	0.566187	0.51693186	0.8203	0.634472805	6
15	0.897713	0.83898974	1	0.102287166	0.16101026	0	0.830169	0.75641791	1	0.862195562	3
16	0.952986	0.94238358	0.91075051	0.047013977	0.057616417	0.089249	0.914053	0.89667374	0.848537	0.886421392	2

Table 6 Grey-fuzzy grade (GFG) and rank of the experiments

Test	GFG	Rank
1	0.420	13
2	0.383	15
3	0.462	11
4	0.568	7
5	0.364	16
6	0.410	14
7	0.498	9
8	0.634	6
9	0.422	12
10	0.540	8
11	0.685	4
12	0.878	1
13	0.479	10
14	0.635	5
15	0.789	2
16	0.761	3

fuel-bound nitrogen oxides and sulfur oxides is also less (Mumbach et al. 2019). The oxygen content is approximately 2.86% which is a matter of concern because higher oxygen can lead to a higher formation of nitrogen oxides (in the context of engine application) which is contagious and not good for the environment. However, higher oxygen content on the other hand can de-promote the smoke formation during the diffusion combustion phase in an internal combustion engine (Panithasan et al. 2019). In addition, the higher oxygen content of fuel reduces the carbon monoxide and unburnt hydrocarbon emissions

of an engine by oxidizing them into carbon dioxide and water respectively (Khalife et al. 2017). Nevertheless, the promising results in regard to the higher volatile content and hydrocarbon content in WPO extracted from PGB show its potentiality as an alternative to conventional petroleum fuels. The results are similar to the findings of Quesada et al. (2019b) (study on plastic film derived WPO) and Sharma et al. (2014) (study on HDPE grocery bag derived WPO). In this study, the HHV of the PGB derived oil has been found to be 46,685 kJ/kg which is also an added advantage for WPO derived from PGB since higher HHV reduces the fuel consumption of the engine (Geo et al. 2018). The HHV was higher than those of the findings of other researchers for example; Quesada et al. (2019a) (approximately 41,221–46,148 kJ/kg for PE-waste derived WPO) and Ahmad et al. (2014) (approximately 30,600 kJ/kg for PE derived WPO). Additionally, the HHV was also higher than diesel found in the study by Sharuddin et al. (2017) (44,940 kJ/kg), and Sharuddin et al. (2016) (43,000 kJ/kg). Table 10 also shows the result of the mass–energy assessment. The mass ratio (MR) was approximately 0.79 which means that from 1 mass unit of input feed, 0.79 mass unit of WPO can be extracted at the optimal operating condition. The energy ratio (ER) includes the HHV of the feed and output WPO, the value of ER was approximately 0.89 which indicates that from 1 unit of raw plastic, 0.89 units of energy can be derived, in terms of the energy contained in the WPO. The energy efficiency term (η_{ef}) takes the electricity consumption (EC) into consideration, the η_{ef} was found to be approximately 0.63. Finally, the energy consumption ratio (ECR)
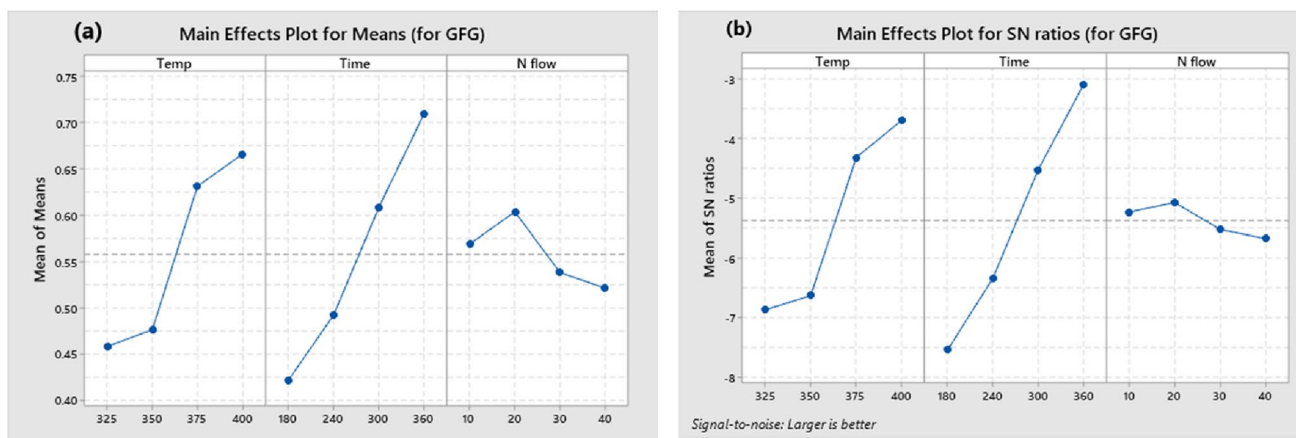
Fig. 4 Comparison of GRG and GFG
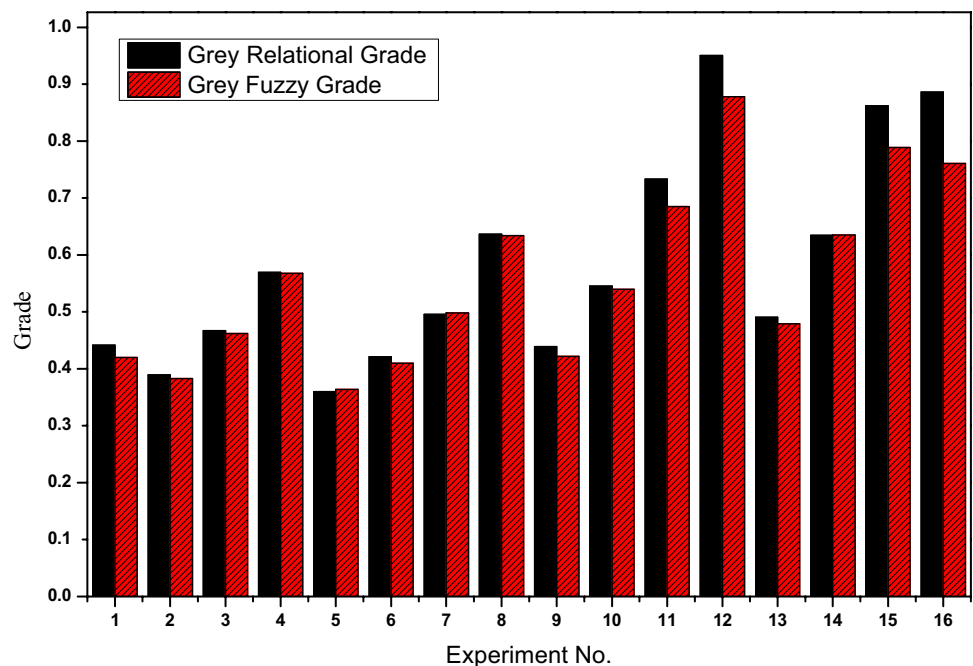
Fig. 5 GFG vs Temperature, Time and N_2 flow rate **a** Main effects plot for means **b** main effects plot for SN ratios

Table 7 Response table for GFG (main effects for means)

Factors	Level 1	Level 2	Level 3	Level 4	Rank	Total mean of GFG
A	0.4582500000	0.4765000000	0.6312500000	**0.6660000000**	2	0.558
B	0.4212500000	0.4920000000	0.6085000000	**0.7102500000**	1	
C	0.5690000000	**0.6035000000**	0.5382500000	0.5212500000	3	

Optimal parameters: **A4-B4-C2**

Table 8 Results of analysis of variance (ANOVA) for GFG

Source	DF	Adj SS	Adj MS	F-Value	P-Value	Remarks	Contribution (%)
Temp	3	0.13449	0.044829	10.1	0.009	Significant	36.15
Time	3	0.19515	0.065049	14.66	0.004	Significant	52.46
N_2 flow	3	0.01573	0.005242	1.18	0.393	Insignificant	4.23
Error	6	0.02663	0.004438				
Total	15	0.37199					

DF: Degree of freedom, SS: Sum of square, MS: Mean square

Table 9 Result of the confirmatory test

Operating condition	Predicted GFG	Experimental GFG	Error (%)
A4-B4-C2	0.81825	0.79751 (With $Y_L = 78.57\%$, $Y_S = 17.93\%$, and $Y_G = 3.5\%$)	2.53

was evaluated and the *ECR* value was less than 1 (0.47), indicating that the pyrolysis process was energy favorable (Guo et al. 2017) since WPO contains more energy than the energy needed for the thermochemical conversion of PGB (Vieira et al. 2020).

FT-IR analysis of WPO

The FT-IR spectra of WPO, extracted at the optimal operating condition, are illustrated in Fig. 6. Table 11 shows major groups and their class of compounds in WPO. The

functional groups determined in WPO are O–H stretching at 3428 cm^{-1} (Vanapalli et al. 2020) likely suggesting the existence of alcoholic group; alkane groups consisting of C-H stretching at 2925 cm^{-1}, C-H stretching at 2857 cm^{-1}, and C–H bending at 1374 cm^{-1}; alkene groups consisting of C=C stretching at 1641 cm^{-1}, C=C stretching at 1460 cm^{-1}, C=C bending at 989 cm^{-1}, C–H bending at 908 cm^{-1}, and C–H bending at 723 cm^{-1} (Quesada et al. 2019b). The identified functional groups are in good agreement with the findings reported by Sharma et al. (2014), and Sharuddin et al. (2017). The peaks/the functional groups present in the WPO are also similar to diesel fuel's functional groups which can

Table 10 Proximate and ultimate analysis, HHV, mass-energy assessment of WPO (at the optimal condition)

Proximate analysis	
Content	Weight (%)
Moisture	0.04
Volatile	99.26
Ash	0.70
Fixed carbon*	–
Ultimate analysis	
Content	Weight (%)
Carbon	81.38
Hydrogen	14.50
Nitrogen	0.35
Sulphur	0.17
Oxygen*	2.86
HHV	
46,685 in kJ/kg	
Mass-energy assessment	
Parameter	Value
MR	0.7857
ER	0.889049506
η_{ef}	0.626608434
ECR	0.471096223

*: calculated by difference

be found in the study reported by Quesada et al. (2019b). It is observed that in WPO, the functional groups are mainly alkane and alkene compounds. The alkanes were produced by intermolecular hydrogen transfer reactions while the β cleavage coupled with the intramolecular hydrogen transfer reactions are accountable for the alkene yields (Rodríguez-Luna et al. 2021) during the PGB pyrolysis. The greater the residence period, the more likelihood of β cleavage reactions (Pan et al. 2021).

GC–MS analysis of WPO

The particular chemical components of WPO were determined via GC–MS analysis. The WPO's GC–MS data are shown in Fig. 7. The major components with a relative area greater than 0.5% are enumerated in Table 12. From Table 12, it can be observed that the major compounds ranged between C_8 and C_{27}. In view of GC–MS results, by and large, a liquid oil can be arranged into three distinct divisions: a light fraction (C_7–C_{11}), a middle fraction (C_{12}–C_{20}), and a heavy fraction (C_{21}–C_{36}) fraction (Pan et al. 2021). The overall results revealed that the WPO predominantly comprises light and middle fractions with a lesser heavy fraction. This shows the suitability of WPO extracted from PGB for engine application as an alternative to conventional fuels. The light fraction and middle fractions were 26.4% and 62.7%, whereas, the heavy fraction was 10.9% approximately. The light fraction's average molecular weight was 145.76 g/mol, and for middle and heavy fractions, the same was 228.56, and 355.86 g/mol, respectively. Further, the overall mean molecular weight of WPO was 220.6 g/mol approximately. The mean molecular weight of WPO is comparable to that of diesel-178.6 g/mol (Soares. 2008) and lesser than the findings of other WPOs reported by Pan
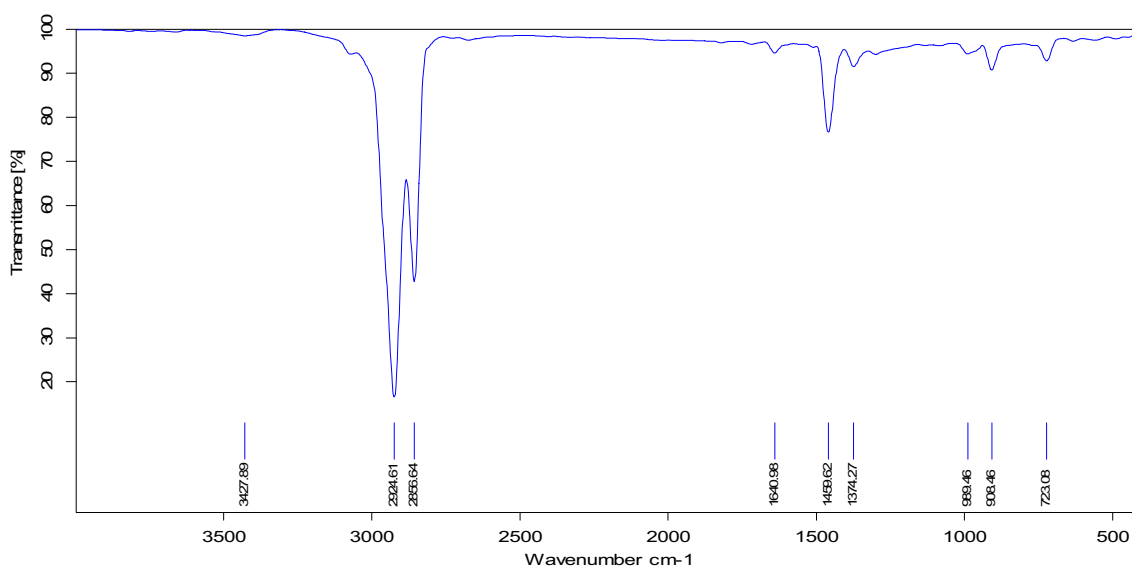
Fig. 6 FT-IR results of WPO

**Table 11** FT-IR spectrometry absorption bands and groups of WPO

Wavelength (cm^{-1})	Group	Class of compound
723.03	C–H bending	Alkenes bands
908.46	C–H bending	Alkene
989.46	C=C bending	Alkene
1374.27	C-H bending	Alkane
1459.62	C=C stretching	Alkene
1640.98	C=C stretching	Alkene
2856.64	C–H stretching	Alkane
2924.61	C–H stretching	Alkane
3427.89	O–H stretching	Alcohol

et al. (291–325.23 g/mol) (Pan et al. 2021), and Quesada et al. (286 g/mol) (Quesada et al. 2019b).

Conclusions

The optimization of process parameters of thermal pyrolysis of PGB has been carried out in this study. Grey–Fuzzy–Taguchi has been used for predicting the optimal operating conditions. Three input factors (temperature, time, and N$_2$ flow rate), each consisting of four variables, have been taken into consideration, and the design of experiments was selected based on Taguchi L-16 orthogonal array. The higher the better approach was considered for Y_L, whereas, for Y_S and Y_G, the lower the better approach was considered. Amongst the initial tests, the 12th experiment offered the highest WPO (Y_L)

yield of 77.54%, whereas, the Y_S and Y_G of the corresponding experiment were approximately 15.54% and 6.92%. However, from the response of the GFGs, it was found that the combination A4-B4-C2 (temperature 400 °C, time 360 min, and N$_2$ flow rate 20 ml/min) may offer a better WPO yield. From the ANOVA of the GFGs, it was found that time is the most significant factor which has a contribution of 52.46% to the response variables. Accordingly, GFG of A4-B4-C2 was predicted, and a confirmatory test was carried out; at that condition, the yield of WPO was found to be 78.57%, and a negligible error (2.53%) was noticed in between predicted and experimental GFG. Therefore, the optimal parametric combination has been found as A4-B4-C2. The WPO extracted from PGB at the optimal parametric condition showed a high hydrocarbon content with an HHV value of 46,685 kJ/kg. The *MR*, *ER* and η_{ef} values for WPO were approximately 0.79, 0.89, and 0.63, and the *ECR* value was less than 1 which indicates the energy favorability condition for PGB pyrolysis. The FT-IR results showed the presence of mainly alkane and alkene functional groups in WPO. In addition, the GC–MS analysis was also performed which revealed that the WPO extracted from PGB contains mainly light and middle fractions (26.4% and 62.7%, respectively) with a lesser heavy fraction (10.9% approximately). The mean molecular weight of WPO was approximately 220.6 g/mol. Finally, it can be concluded the parametric condition A4-B4-C2 can be considered as an optimal one for PGB pyrolysis for the production of WPO which can act as a potential alternative fuel either to supplement or to substitute conventional petroleum fuels.
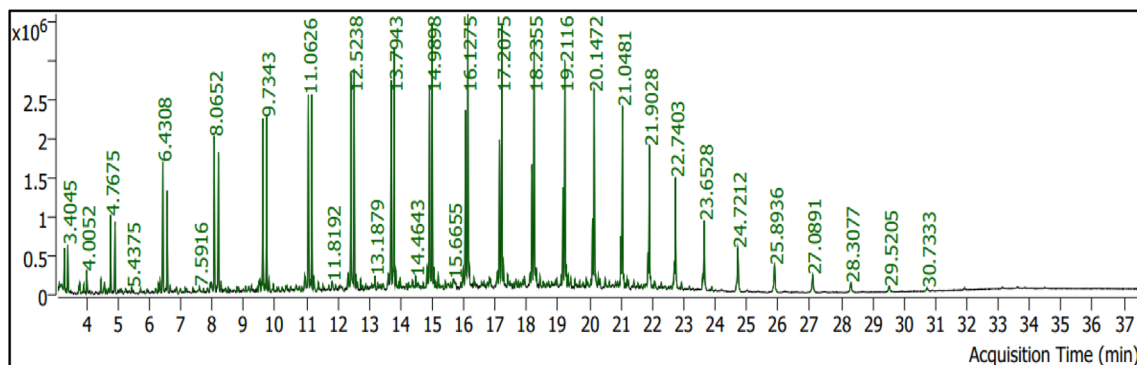
Fig. 7 GC–MS results of WPO

Table 12 Chemical composition of WPO from GC–MS analysis

Major Peak	Chemical compound	Molecular formula	Molecular weight (gm/mol)	Retention time (min)	Content (%)
1	1-Octene	C_8H_{16}	112.1250	3.2948	0.57
2	Octane	C_8H_{18}	114.1410	3.4045	0.60
3	1-Nonene	C_9H_{18}	126.1410	4.7675	1.01
4	Nonane	C_9H_{20}	128.1570	4.9061	0.88
5	1-Decene	$C_{10}H_{20}$	140.1570	6.4308	1.74
6	Decane	$C_{10}H_{22}$	142.1720	6.5694	1.26
7	1-Undecene	$C_{11}H_{22}$	154.1720	8.0652	2.07
8	Undecane	$C_{11}H_{24}$	156.1880	8.1981	1.85
9	1-Dodecene	$C_{12}H_{24}$	168.1880	9.6130	2.34
10	Dodecane	$C_{12}H_{26}$	170.2030	9.7343	2.28
11	1-Tridecene	$C_{13}H_{26}$	182.2030	11.0626	2.68
12	Tridecane	$C_{13}H_{28}$	184.2190	11.1723	2.57
13	1-Tetradecene	$C_{14}H_{28}$	196.2190	12.4198	3.04
14	Tetradecane	$C_{14}H_{30}$	198.2350	12.5238	2.94
15	1-Tridecene	$C_{13}H_{26}$	182.2030	3.6961	2.93
16	Pentadecane	$C_{15}H_{32}$	212.2500	13.7943	3.50
17	Cetene	$C_{16}H_{32}$	224.2500	14.9032	2.91
18	Hexadecane	$C_{16}H_{34}$	226.2660	14.9898	3.69
19	n-Heptadecanol-1	$C_{17}H_{36}O$	256.2770	16.0467	2.59
20	Heptadecane	$C_{17}H_{36}$	240.2820	16.1275	3.57
21	1-Octadecanol	$C_{18}H_{38}O$	270.2920	17.1324	2.15
22	Octadecane	$C_{18}H_{38}$	254.2970	17.2075	3.68
23	1-Nonadecene	$C_{19}H_{38}$	266.2970	18.1662	1.78
24	Nonadecane	$C_{19}H_{40}$	268.3130	18.2355	3.48
25	3-Eicosene, (E)-	$C_{20}H_{40}$	280.3130	19.1538	1.41
26	Eicosane	$C_{20}H_{42}$	282.3290	19.2116	3.21
27	1-Nonadecene	$C_{19}H_{38}$	266.2970	20.0952	1.00
28	Heneicosane	$C_{21}H_{44}$	296.3440	20.1472	2.91
29	Behenic alcohol	$C_{22}H_{46}O$	326.3550	20.9961	0.72
30	Docosane	$C_{22}H_{46}$	310.3600	21.0481	2.66
31	1-Octadecanol	$C_{18}H_{38}O$	270.2920	21.8624	0.53
32	Heptacosane	$C_{27}H_{56}$	380.4380	21.9028	2.24
33	Tetracosane	$C_{24}H_{50}$	338.3910	22.7403	1.75
34	Heptacosane	$C_{27}H_{56}$	380.4380	23.6528	1.25
35	Heptacosane	$C_{27}H_{56}$	380.4380	24.7212	1.11
36	Heptacosane	$C_{27}H_{56}$	380.4380	25.8936	0.75
37	Heptacosane	$C_{27}H_{56}$	380.4380	27.0891	0.51

Declarations

Conflict of interest The authors declare that they have no conflict of interest.

References

Ahmad I, Khan MI, Khan H, Ishaq M, Tariq R, Gul K, Ahmad W (2014) Pyrolysis study of polypropylene and polyethylene into premium oil products. Int J Green Energy 12:663–671. https://doi.org/10.1080/15435075.2014.880146

Awale A, Inamdar K (2020) Multi-objective optimization of high-speed turning parameters for hardened AISI S7 tool steel using grey relational analysis. J Braz Soc Mech Sci Eng. https://doi.org/10.1007/s40430-020-02433-z

Bharathy S, Gnanasikamani B, Lawrence KR (2019) Investigation on the use of plastic pyrolysis oil as alternate fuel in a direct injection diesel engine with titanium oxide nanoadditive. Environ Sci Pollut Res 26:10319–10332. https://doi.org/10.1007/s11356-019-04293-0

Bhowmik A, Biswas A (2021) Wear resistivity of Al7075/6wt%SiC composite by using grey-fuzzy optimization technique. SILICON. https://doi.org/10.1007/s12633-021-01160-x

Cai J, He Y, Yu X, Banks SW, Yang Y, Zhang X, Yu Y, Liu R, Bridgwater AV (2017) Review of physicochemical properties and analytical characterization of lignocellulosic biomass. Renew Sustain Energy Rev 76:309–322. https://doi.org/10.1016/j.rser.2017.03.072

Central Pollution Control Board (CPCB) (2018) Annual report on plastic waste management rule. CPCB Ministry of Environment, Forest and Climate Change, Govt. of India, Delhi. http://cpcb.nic.in/uploads/plasticwaste/Annual_Report_2017-18_PWM.pdf

Dauvergne P (2018) Why is the global governance of plastic failing the oceans? Glob Environ Chang 51:2–31. https://doi.org/10.1016/j.gloenvcha.2018.05.002

Dey S, Deb M, Das PK (2019) Application of fuzzy-assisted grey Taguchi approach for engine parameters optimization on performance-emission of a CI engine. Energy Sour Part A Recover Util Environ Eff. https://doi.org/10.1080/15567036.2019.1697392

EUNOMIA (2018) Plastic Packaging. Shredding Light on the UK Data- A Report by Eunomia Research & Consulting Ltd, Bristol, UK. https://www.eunomia.co.uk/reports-tools/plastic-packaging-shedding-light-on-the-uk-data/ (Accessed on 20th December 2021)

Geo VE, Sonthalia A, Aloui F, Js FJ (2018) Study of engine performance, emission and combustion characteristics fueled with diesel-like fuel produced from waste engine oil and waste plastics. Front Environ Sci Eng. https://doi.org/10.1007/s11783-018-1063-6

Guo F, Wang X, Yang X (2017) Potential pyrolysis pathway assessment for microalgae-based aviation fuel based on energy conversion efficiency and life cycle. Energy Convers Manage 132:272–280. https://doi.org/10.1016/j.enconman.2016.11.020

Insura N, Onwudili JA, Williams PT (2010) Catalytic pyrolysis of low-density polyethylene over alumina-supported noble metal catalysts. Energy Fuels 24:4231–4240. https://doi.org/10.1021/ef100227f

Jozić S, Bajić D, Celent L (2015) Application of compressed cold air cooling: achieving multiple performance characteristics in end milling process. J Clean Prod 100:325–332. https://doi.org/10.1016/j.jclepro.2015.03.095

Kalargaris I, Tian G, Gu S (2017) Experimental evaluation of a diesel engine fuelled by pyrolysis oils produced from low-density polyethylene and ethylene–vinyl acetate plastics. Fuel Process Technol 161:125–131. https://doi.org/10.1016/j.fuproc.2017.03.014

Khalife E, Tabatabaei M, Demirbas A, Aghbashlo M (2017) Impacts of additives on performance and emission characteristics of diesel engines during steady state operation. Progr Energy Combust Sci 59:32–78. https://doi.org/10.1016/j.pecs.2016.10.001

Khamparia A, Pandey B, Pandey DK, Gupta D, Khanna A, de Albuquerque VHC (2020) Comparison of RSM, ANN and fuzzy logic for extraction of oleonolic acid from ocimum sanctum. Comput Ind 117:103200. https://doi.org/10.1016/j.compind.2020.103200

Lin JL, Lin CL (2005) The use of grey-fuzzy logic for the optimization of the manufacturing process. J Mater Process Technol 160:9–14. https://doi.org/10.1016/j.jmatprotec.2003.11.040

Mastral FJ, Esperanza E, Garcia P, Juste M (2002) Pyrolysis of high-density polyethylene in a fluidised bed reactor. Influence of the temperature and residence time. J Anal Appl Pyrolysis 63:1–15. https://doi.org/10.1016/S0165-2370(01)00137-1

Miskolczi N, Bartha L, Deák G, Jóver B, Kalló D (2004) Thermal and thermo-catalytic degradation of high-density polyethylene waste. J Anal Appl Pyrol 72:235–242. https://doi.org/10.1016/j.jaap.2004.07.002

Muhammad I, Makwashi N, Manos G (2018) Catalytic degradation of linear low-density polyethylene over hy-zeolite via pre-degradation method. J Anal Appl Pyrol. https://doi.org/10.1016/j.jaap.2018.11.025

Mumbach GD, Alves JLF, Silva JCGD, Sena RFD, Marangoni C, Machado RAF, Bolzan A (2019) Thermal investigation of plastic solid waste pyrolysis via the deconvolution technique using the asymmetric double sigmoidal function: determination of the kinetic triplet, thermodynamic parameters, thermal lifetime and pyrolytic oil composition for clean energy recovery. Energy Convers Manage 200:112031. https://doi.org/10.1016/j.enconman.2019.112031

Onwudili JA, Insura N, Williams PT (2009) Composition of products from the pyrolysis of polyethylene and polystyrene in a closed batch reactor: effects of temperature and residence time. J Anal Appl Pyrol 86:293–303. https://doi.org/10.1016/j.jaap.2009.07.008

Our World in Data (2018) Plastic Pollution. https://ourworldindata.org/plastic-pollution (Accessed on 20th December 2021)

Pan R, Martins MF, Debenest G (2021) Pyrolysis of waste polyethylene in a semi-batch reactor to produce liquid fuel: Optimization of operating conditions. Energy Convers Manage 237:114114. https://doi.org/10.1016/j.enconman.2021.114114

Panda A, Sahoo AK, Rout AK (2016) Multi-attribute decision making parametric optimization and modeling in hard turning using ceramic insert through grey relational analysis: a case study. Decis Sci Lett 5:581–592. https://doi.org/10.5267/j.dsl.2016.3.001

Pandey AK, Gautam GD (2018) Grey relational analysis-based genetic algorithm optimization of electrical discharge drilling of Nimonic-90 superalloy. J Braz Soc Mech Sci Eng 40:117. https://doi.org/10.1007/s40430-018-1045-4

Panithasan MS, Gopalakichenin D, Venkadesan G, Veeraraagavan S (2019) Impact of rice husk nanoparticle on the performance and emission aspects of a diesel engine running on blends of pine oil-diesel. Environ Sci Pollut Res 26:282–291. https://doi.org/10.1007/s11356-018-3601-y

Paramasivam B (2020) Fuzzy prediction and RSM optimization of CI engine performance analysis: aegle marmelos non-edible seed cake pyrolysis oil as a diesel alternative. Energy Sour Part A Recover Util Environ Eff. https://doi.org/10.1080/15567036.2020.1773971

Quesada L, Pérez A, Godoy V, Peula FJ, Calero M, Blázquez G (2019a) Optimization of the pyrolysis process of a plastic waste to obtain a liquid fuel using different mathematical models. Energy Convers

Manage 188:19–26. https://doi.org/10.1016/j.enconman.2019.03.054

Quesada L, Calero M, Martín-Lara MA, Pérez A, Blázquez G (2019b) Characterization of fuel produced by pyrolysis of plastic film obtained of municipal solid waste. Energy 186:115874. https://doi.org/10.1016/j.energy.2019b.115874

Rodríguez-Luna L, Bustos-Martínez D, Valenzuela E (2021) Two-step pyrolysis for waste HDPE valorization. Process Saf Environ Prot 149:526–536. https://doi.org/10.1016/j.psep.2020.11.038

Roy S, Das AK, Banerjee R (2016) Grey-Fuzzy Taguchi approach for multi-objective optimization of performance and emission parameters of a single cylinder CRDI engine coupled with EGR. Int J Automot Technol 17:1–12. https://doi.org/10.1007/s12239-016-0001-5

Saha D, Sinha A, Pattanayak S, Roy B (2021a) Pyrolysis kinetics and thermodynamic parameters of plastic grocery bag based on thermogravimetric data using iso-conversional methods. Int J Environ Sci Technol. https://doi.org/10.1007/s13762-020-03106-z

Saha D, Sinha A, Roy B (2021b) Critical insights into the effects of plastic pyrolysis oil on emission and performance characteristics of CI engine. Environ Sci Pollut Res 28:44598–44621. https://doi.org/10.1007/s11356-021-14919-x

Sharma BK, Moser BR, Vermillion KE, Doll KM, Rajagopalan N (2014) Production, characterization and fuel properties of alternative diesel fuel from pyrolysis of waste plastic grocery bags. Fuel Process Technol 122:79–90. https://doi.org/10.1016/j.fuproc.2014.01.019

Sharuddin SDA, Abnisa F, Daud WMAW, Aroua MK (2016) A review on pyrolysis of plastic wastes. Energy Convers Manage 115:308–326. https://doi.org/10.1016/j.enconman.2016.02.037

Sharuddin SDA, Abnisa F, Daud WMAW, Aroua MK (2017) Energy recovery from pyrolysis of plastic waste: Study on non-recycled plastics (NRP) data as the real measure of plastic waste. Energy Convers Manage 148:925–934. https://doi.org/10.1016/j.enconman.2017.06.046

Singh RK, Ruj B, Sadhukhan AK, Gupta P (2019) Thermal degradation of waste plastics under non-sweeping atmosphere: part 1: effect of temperature, product optimization, and degradation mechanism. J Environ Manage 239:395–406. https://doi.org/10.1016/j.jenvman.2019.03.067

Singh RK, Ruj B, Sadhukhan AK, Gupta P (2020) Thermal degradation of waste plastics under non-sweeping atmosphere: part 2: effect of process temperature on product characteristics and their future applications. J Environ Manage 261:110112. https://doi.org/10.1016/j.jenvman.2020.110112

Soares C (2008) Gas turbine fuel systems and fuels. Gas Turbines. https://doi.org/10.1016/b978-075067969-5.50012-0

The world counts (2021) https://www.theworldcounts.com/challenges/planet-earth/waste/plastic-bags-used-per-year/story (Accessed on 20th December 2021)

Tiikma L, Tamvelius H, Luik L (2007) Coprocessing of heavy shale oil with polyethylene waste. J Anal Appl Pyrol 79:191–195. https://doi.org/10.1016/j.jaap.2006.12.029

Vanapalli KR, Bhattacharya J, Samal B, Chandra S, Medha I, Dubey BK (2020) Optimized production of Single-use plastic-Eucalyptus wood char composite for application in soil. J Clean Prod 79:191–195. https://doi.org/10.1016/j.jclepro.2020.123968

Venkatesan H, Sivamani S, Bhutoria K, Vora HH (2018) Experimental study on combustion and performance characteristics in a DI CI engine fuelled with blends of waste plastic oil. Alex Eng J 57:2257–2263. https://doi.org/10.1016/j.aej.2017.09.001

Vieira FR, Luna CMR, Arce GLAF, Ávila I (2020) Optimization of slow pyrolysis process parameters using a fixed bed reactor for biochar yield from rice husk. Biomass Bioenerg 132:105412. https://doi.org/10.1016/j.biombioe.2019.105412

Wirawan RP, Farizal (2019) Plastic waste pyrolysis optimization to produce fuel grade using factorial design. E3S Web of Conferences 125:13005. https://doi.org/10.1051/e3sconf/201912513005

Zhang Y, Ji G, Ma D, Chen C, Wang Y, Wang W, Li A (2020) Exergy and energy analysis of pyrolysis of plastic wastes in rotary kiln with heat carrier. Process Saf Environ Prot 142:203–211. https://doi.org/10.1016/j.psep.2020.06.021